EUROPEAN ORGANIZATION FOR NUCLEAR RESEARCH (CERN)

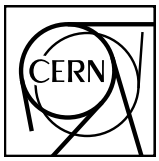

CERN-EP-2021-176
24 August 2021

Study of Z bosons produced in association with charm in the forward region

LHCb collaboration[†]

Abstract

The fraction of Z+jet events that contain a charm jet is measured for the first time in the forward region of proton-proton collisions. The data sample used corresponds to an integrated luminosity of $6\,\text{fb}^{-1}$ collected at a center-of-mass energy of 13 TeV with the LHCb detector. The ratio of production cross sections $\sigma(Zc)/\sigma(Zj)$ is determined in intervals of Z-boson rapidity in the range $2.0 < y(Z) < 4.5$. A sizable enhancement is observed in the forward-most $y(Z)$ interval, which could be indicative of a valence-like intrinsic-charm component in the proton wave function.

Submitted to Physical Review Letters

[†]Authors are listed at the end of this Letter.

The possibility that the proton wave function may contain a $|uudc\bar{c}\rangle$ component, referred to as intrinsic charm (IC), in addition to the charm content that arises due to perturbative gluon radiation, *i.e.* $g \to c\bar{c}$ splitting, has been debated for decades (for a recent review, see Ref. [1]). Light front QCD (LFQCD) calculations predict that non-perturbative IC manifests as valence-like charm content in the parton distribution functions (PDFs) of the proton [2, 3]; whereas, if the c-quark content is entirely perturbative in nature, the charm PDF resembles that of the gluon and sharply decreases at large momentum fractions, x. Understanding the role that non-perturbative dynamics play inside the nucleon is a fundamental goal of nuclear physics [4–14]. Furthermore, the existence of IC would have many phenomenological consequences. For example, IC would alter both the rate and kinematics of c hadrons produced by cosmic-ray proton interactions in the atmosphere; the subsequent semileptonic decays of such c hadrons are an important source of background in studies of astrophysical neutrinos [15–20]. The cross sections of many processes at the LHC and other accelerators would also be affected [21–31].

Measurements of c-hadron production in deep inelastic scattering [32] and in fixed-target experiments [33], where the typical momentum transfers were $Q \lesssim 10\,\text{GeV}$ (natural units are used throughout this Letter), have been interpreted both as evidence for [34, 35] and against [36] the percent-level IC content predicted by LFQCD. Even though such experiments are in principle sensitive to valence-like c-quark content, interpreting these low-Q data is challenging since it requires careful theoretical treatment of hadronic and nuclear effects. Recent global PDF analyses, which also include measurements from the LHC, are inconclusive and can only exclude IC carrying more than a few percent of the momentum of the proton [37, 38].

Reference [28] proposed studying IC by measuring the fraction of Z-boson+jet events that contain a charm jet, $\mathcal{R}_j^c \equiv \sigma(Zc)/\sigma(Zj)$, in the forward region of proton-proton (pp) collisions at the LHC. The ratio $\mathcal{R}_j^c$ was chosen because it is less sensitive than $\sigma(Zc)$ to experimental and theoretical uncertainties. Since Zc production is inherently at large Q, above the electroweak scale, hadronic effects are small. A leading-order Zc production mechanism is $gc \to Zc$ scattering (see Fig. 1), where in the forward region one of the initial partons must have large x, hence Zc production probes the valence-like region. Using next-to-leading-order (NLO) Standard Model (SM) calculations, Fig. 2 illustrates that a percent-level valence-like IC contribution would produce a clear enhancement in $\mathcal{R}_j^c$ for large (more forward) values of Z rapidity, $y(Z)$; whereas only small effects are expected in the central region where all previous measurements of $\mathcal{R}_j^c$ were made [39, 40].

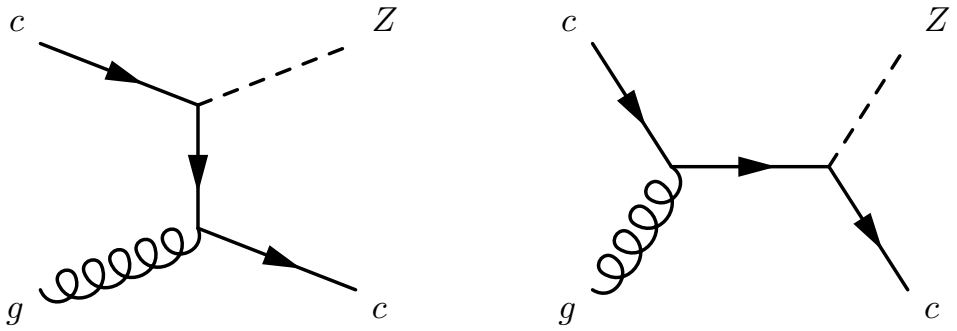

Figure 1: Leading-order Feynman diagrams for $gc \to Zc$ production.

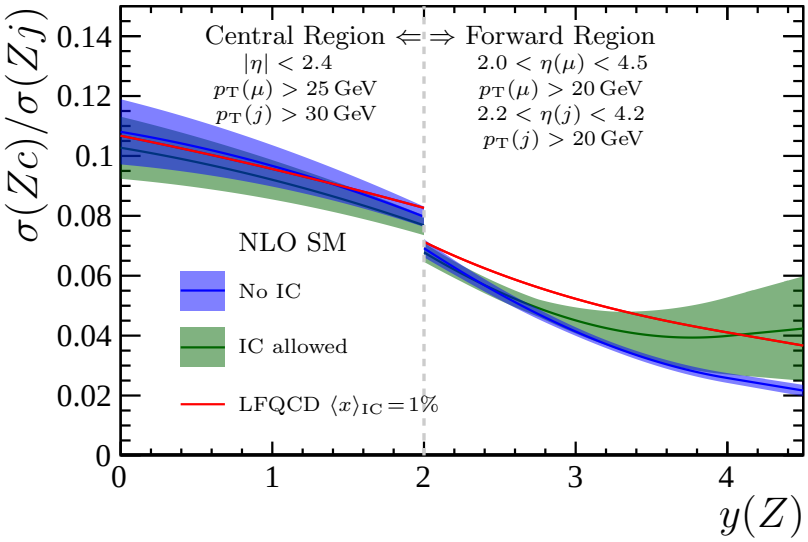

Figure 2: NLO SM predictions [28] for $\mathcal{R}_j^c$ without IC [41], allowing for potential IC [38], and with the valence-like IC predicted by LFQCD with a mean momentum fraction of 1% [37]. The fiducial region from Ref. [40] is used for $y(Z) < 2$; otherwise the fiducial region of this analysis is employed. The broadening of the error band that arises in the forward region, when allowing for IC, is due to the lack of sensitivity to valence-like IC from previous experiments. More details on these calculations are provided in the Supplemental Material [42].

Table 1: Definition of the fiducial region.

Z bosons	$p_T(\mu) > 20\,\text{GeV}$, $2.0 < \eta(\mu) < 4.5$, $60 < m(\mu^+\mu^-) < 120\,\text{GeV}$
Jets	$20 < p_T(j) < 100\,\text{GeV}$, $2.2 < \eta(j) < 4.2$
Charm jets	$p_T(c\text{ hadron}) > 5\,\text{GeV}$, $\Delta R(j, c\text{ hadron}) < 0.5$
Events	$\Delta R(\mu, j) > 0.5$

This Letter presents the first measurement of $\mathcal{R}_j^c$ in the forward region of pp collisions. The data sample used corresponds to an integrated luminosity of $6\,\text{fb}^{-1}$ collected at a center-of-mass energy of $\sqrt{s} = 13\,\text{TeV}$ with the LHCb detector. The Z bosons are reconstructed using the $Z \to \mu^+\mu^-$ decay, where henceforth all $Z/\gamma^* \to \mu^+\mu^-$ production in the mass range $60 < m(\mu^+\mu^-) < 120\,\text{GeV}$ is labeled $Z \to \mu^+\mu^-$. The analysis is performed using jets clustered with the anti-k_T algorithm [43] using a distance parameter $R = 0.5$. The fiducial region is defined in terms of the transverse momentum, p_T, pseudorapidity, η, and azimutal angle, ϕ, of the muon and jet momenta, and includes a requirement on $\Delta R(\mu, j) \equiv \sqrt{\Delta\eta(\mu, j)^2 + \Delta\phi(\mu, j)^2}$ to ensure that the muons and jet are well separated, which suppresses backgrounds from QCD multijet events and electroweak processes like W+jet production. Charm jets are the subset for which there is a promptly produced and weakly decaying c hadron within the jet. The fiducial region is defined in Table 1. If multiple jets satisfy these criteria, the one with the highest p_T is selected.

The quantity $\mathcal{R}_j^c$ is measured in intervals of $y(Z)$ as $\mathcal{R}_j^c = N(c\text{-tag})/[\varepsilon(c\text{-tag})N(j)]$, where $N(c\text{-tag})$ is the observed Zc yield, $\varepsilon(c\text{-tag})$ is the c-tagging efficiency, and $N(j)$ is the total Zj yield. The integrated luminosity does not enter this expression because $\mathcal{R}_j^c$

involves a ratio of production cross sections. In addition, the muon and jet reconstruction efficiencies largely cancel in the ratio due to the similarity of the Z-boson and jet kinematics in Zc and Zj production. The c-tagging algorithm, which is described in detail in Ref. [44], looks for a displaced-vertex (DV) signature inside the jet cone that is indicative of the weak decay of a c hadron.

The LHCb detector is a single-arm forward spectrometer covering the pseudorapidity range $2 < \eta < 5$, described in detail in Refs. [45, 46]. Simulated data samples are used to evaluate the detector response for jet reconstruction, including the c-tagging efficiency, and to validate the analysis. In the simulation, pp collisions are generated using Pythia [47] with a specific LHCb configuration [48]. Decays of unstable particles are described by EvtGen [49], in which final-state radiation is generated using Photos [50]. The interaction of the generated particles with the detector, and its response, are implemented using the Geant4 toolkit [51] as described in Ref. [52].

The online event selection is performed by a trigger [53, 54] consisting of a hardware stage using information from the calorimeter and muon systems, followed by a software stage that performs a full event reconstruction. At the hardware stage, events are required to have a muon with $p_{\mathrm{T}}(\mu) > 6\,\mathrm{GeV}$. In the software stage, the muon track is required to be of good quality and to have $p_{\mathrm{T}}(\mu) > 10\,\mathrm{GeV}$. The offline selection builds $Z \to \mu^+\mu^-$ candidates from two oppositely charged muon tracks that must be in the fiducial region defined in Table 1 and consistent with originating directly from the same pp collision.

Jet reconstruction is performed offline by clustering charged and neutral particle-flow candidates [55] using the anti-k_{T} clustering algorithm as implemented in FastJet [56]. Reconstructed jets with $15 < p_{\mathrm{T}}(j) < 100\,\mathrm{GeV}$ and $2.2 < \eta(j) < 4.2$ are kept for further analysis. Jets with $15 < p_{\mathrm{T}}(j) < 20\,\mathrm{GeV}$, which are outside of the fiducial region, are retained for use when unfolding the detector response. The $\eta(j)$ requirement, which is included in the fiducial region and was first used in Refs. [57–59], ensures a nearly uniform c-tagging efficiency of about 24%, with minimal $p_{\mathrm{T}}(j)$ or $\eta(j)$ dependence. The fiducial requirement $\Delta R(\mu, j) > 0.5$ is applied to reconstructed jets. Finally, the highest-p_{T} jet satisfying these criteria from the same pp collision as the Z boson is selected. After applying all requirements, 68 694 Zj candidates remain in the dataset.

The effects of the detector response on the measured jet momenta are accounted for using an unfolding procedure. This involves first determining the reconstructed Zc and Zj yields in intervals of $[y(Z), p_{\mathrm{T}}(j)]$. The non-$Z$ background is neglected for both Zc and Zj candidates because it is less than 1% and largely cancels in the $\mathcal{R}_j^c$ ratio. The c-jet yields are determined using the DV-based tagging approach described in detail in the following paragraphs. Interval migration is accounted for by unfolding the $p_{\mathrm{T}}(j)$ distributions of the Zc and Zj yields in each $y(Z)$ interval independently using an iterative Bayesian procedure [60, 61]. The Zc yields are then corrected for c-tagging inefficiency. Finally, the unfolded $[y(Z), p_{\mathrm{T}}(j)]$ distributions are integrated for $p_{\mathrm{T}}(j) > 20\,\mathrm{GeV}$ to obtain the Zc and Zj yields used to determine the $\mathcal{R}_j^c$ ratios. The analysis employs three $y(Z)$ intervals with ranges 2.00–2.75, 2.75–3.50, and 3.50–4.50, and four $p_{\mathrm{T}}(j)$ intervals ranging 15–20, 20–30, 30–50, and 50–100 GeV, where after unfolding the yields in the three highest $p_{\mathrm{T}}(j)$ intervals are summed to obtain $\mathcal{R}_j^c$.

The signature of a c jet is the presence of a long-lived c hadron that carries a sizable fraction of the jet energy. The tagging of c jets is performed using DVs formed from the decays of such c hadrons. The choice of using DVs and not single-track or other non-DV-based jet properties, *e.g.* the number of particles in the jet, is driven by the need

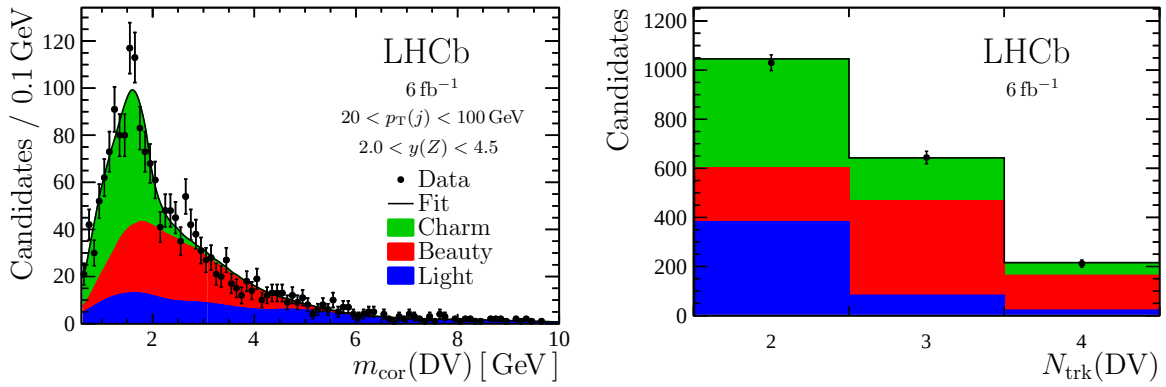

Figure 3: Distributions of (left) $m_{\rm cor}(\rm DV)$ and (right) $N_{\rm trk}(\rm DV)$ for all DV-tagged candidates in the Zj data sample reconstructed in the fiducial region with the projections of the fit results superimposed.

for a small misidentification probability of light-parton jets. Furthermore, the properties of DVs from c-hadron decays are known to be well modeled by simulation, which means that only small corrections using control samples are required. Since DVs can also be formed from the decays of b hadrons or due to artifacts of the reconstruction, the DV-tagged charm yields are obtained by fitting the distributions of DV features with good discrimination power between c, b, and light-parton jets.

The tracks used as inputs to the DV-tagger algorithm are required to have $p_{\rm T} > 0.5\,\rm GeV$ and to be inconsistent with originating directly from a pp collision. A DV is associated to a jet when $\Delta R < 0.5$ between the jet axis and the DV direction of flight, defined by the vector from the pp interaction point to the DV position. Requirements that reject strange-hadron decays and particles formed in interactions with material [62] are placed on the mass, $m(\rm DV)$, and momentum, $p(\rm DV)$, of the particles that form the DV, along with the DV position. In addition, only DVs with at most four tracks are used, since higher-multiplicity DVs are almost exclusively due to b-hadron decays. More details about the c-tagging algorithm are provided in Ref. [44].

Two DV properties are used to separate charm jets from beauty and light-parton jets: the number of tracks in the DV, $N_{\rm trk}(\rm DV)$, and the corrected mass, $m_{\rm cor}(\rm DV) \equiv \sqrt{m(\rm DV)^2 + [p(\rm DV)\sin\theta]^2} + p(\rm DV)\sin\theta$, where θ is the angle between the momentum and the flight direction of the DV. The corrected mass, which is the minimum mass the long-lived hadron can have that is consistent with the flight direction, peaks near the typical c-hadron mass for c jets, and consequently provides excellent discrimination against other jet types. The DV track multiplicity provides additional discrimination against b jets, since b-hadron decays often produce many displaced tracks. These two distributions are fitted simultaneously to obtain the DV-tagged c-jet yields. The probability density functions, referred to as templates, for c, b, and light-parton jets are obtained from calibration data samples that are each highly enriched in a given jet flavor [44]. Figure 3 shows the $m_{\rm cor}(\rm DV)$ and $N_{\rm trk}(\rm DV)$ distributions for all DV-tagged candidates in the Zj data sample reconstructed in the fiducial region, along with the fit projections; such fits are performed in each $[y(Z), p_{\rm T}(j)]$ interval to obtain the reconstructed Zc yields.

The effects of $p_{\rm T}(j)$ interval migration are corrected for using the unfolding procedure. The detector response is studied using the $p_{\rm T}$-balance distribution $p_{\rm T}(j)/p_{\rm T}(Z)$ for Zj

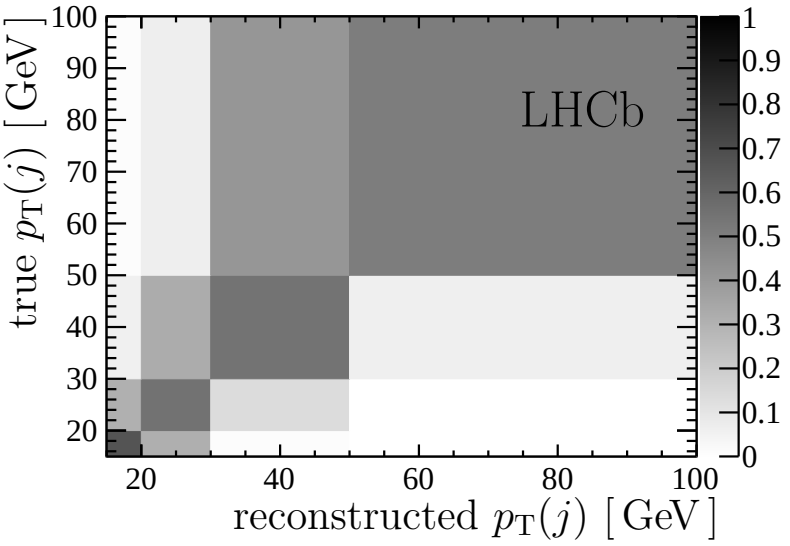

Figure 4: The detector-response matrix for c-tagged jets. The shading represents the interval-to-interval migration probabilities ranging from (white) 0 to (black) 1. Jets with true (reconstructed) $p_{\rm T}(j)$ in the 20–100 GeV region but for which the reconstructed (true) $p_{\rm T}(j)$ is either below 15 GeV or above 100 GeV are included in the unfolding but not shown graphically.

candidates that are nearly back-to-back in the transverse plane, using the same technique as in Refs. [55, 63]. Small adjustments are applied to the $p_{\rm T}(j)$ scale and resolution in simulation to obtain the best agreement with data. In addition, for the Zc and Zj samples the $p_{\rm T}(j)$ and $p_{\rm T}({\rm DV})$ distributions in simulation are adjusted to match those observed in data. The unfolding matrix for jets that contain a reconstructed DV is shown in Fig. 4, while the corresponding matrix for inclusive Zj production is provided in the Supplemental Material [42].

The dominant systematic uncertainty is due to limited knowledge of the c-tagging efficiency, which is measured in $p_{\rm T}(j)$ intervals using data in Ref. [44] and briefly summarized here. Scale factors that correct for discrepancies between data and simulation are determined using a tag-and-probe approach on a dijet calibration sample. A stringent requirement is applied to the tag jet which enriches the probe-jet sample in charm content. The DV-tagged c-jet yield in the probe sample is obtained in the same way the Zc yield is determined in this analysis, namely by fitting the $m_{\rm cor}({\rm DV})$ and $N_{\rm trk}({\rm DV})$ distributions for DV-tagged probe jets. The total number of c jets in the probe sample is obtained by fully reconstructing the $D^0 \to K^-\pi^+$ and $D^+ \to K^-\pi^+\pi^+$ decays, obtaining the prompt-charm yields by fitting the D-meson mass and impact-parameter distributions, then correcting these yields for the detector response, decay branching fractions [64], and c-hadron fragmentation fractions [65]. The c-tagging efficiency is the ratio of the DV-tagged and total c-jet probe-sample yields. The scale factors that correct the c-tagging efficiency in simulation are determined to be 1.03 ± 0.06, 1.01 ± 0.08, and 1.09 ± 0.17 in the 20–30, 30–50, and 50–100 GeV $p_{\rm T}(j)$ intervals, respectively, with corresponding c-tagging efficiencies of $(23.9 \pm 1.4)\%$, $(24.4 \pm 1.9)\%$, and $(23.6 \pm 4.1)\%$. These uncertainties, which include all statistical and systematic contributions, are propagated to the $\mathcal{R}_j^c$ results producing 6–7% relative uncertainties in each $y(Z)$ interval.

Other sources of smaller systematic uncertainty are also considered. First, variations

Table 2: Relative systematic uncertainties on $\mathcal{R}_j^c$, where ranges indicate that the value depends on the $y(Z)$ intervals.

Source	Relative Uncertainty
c tagging	6–7%
DV-fit templates	3–4%
Jet reconstruction	1%
Jet p_{T} scale & resolution	1%
Total	8%

Table 3: Numerical results for the $\mathcal{R}_j^c$ measurements, where the first uncertainty is statistical and the second is systematic.

$y(Z)$	$\mathcal{R}_j^c$ (%)
2.00–2.75	$6.84 \pm 0.54 \pm 0.51$
2.75–3.50	$4.05 \pm 0.32 \pm 0.31$
3.50–4.50	$4.80 \pm 0.50 \pm 0.39$
2.00–4.50	$4.98 \pm 0.25 \pm 0.35$

of the $m_{\mathrm{cor}}(\mathrm{DV})$ and $N_{\mathrm{trk}}(\mathrm{DV})$ templates are studied, which arise from using different strategies to model the backgrounds in the highly enriched calibration data samples. However, the shifts observed in the Zc yields largely cancel with the corresponding shifts seen in $\varepsilon(c\text{-tag})$. The residual differences of 3–4% in each $y(Z)$ interval are assigned as systematic uncertainties. The ratio of the jet-reconstruction efficiency for c and inclusive jets is consistent with unity in all kinematic intervals in simulation, with a 1% systematic uncertainty assigned due to the limited sample sizes. Finally, the statistical precision of the back-to-back Zj sample used to determine the $p_{\mathrm{T}}(j)$ scale and resolution is propagated through the unfolding procedure resulting in a 1% relative systematic uncertainty on $\mathcal{R}_j^c$. The systematic uncertainties are summarized in Table 2.

Figure 5 shows the measured $\mathcal{R}_j^c$ distribution in intervals of $y(Z)$; the numerical results are provided in Table 3, and additional results are reported in the Supplemental Material [42]. The measured $\mathcal{R}_j^c$ values are compared to NLO SM calculations [28] based on Refs. [66–72], which are validated against additional predictions [69,70,73,74] and updated here to use more recent PDFs [37,38,41,75,76]. The NNPDF analysis provides results where the charm PDF is allowed to vary, both in size and in shape [38]. Reference [37] updated the CT14 analysis [77] to include the IC content predicted by LFQCD [2,3], which results in the enhancement at forward $y(Z)$ shown previously in Fig. 2. More details on the theory calculations are provided in the Supplemental Material [42].

The observed $\mathcal{R}_j^c$ values are consistent with both the no-IC and IC hypotheses in the first two $y(Z)$ intervals; however, this is not the case in the forward-most interval where the ratio of the observed to no-IC-expected values is 1.85 ± 0.25. As illustrated in Fig. 2, this is precisely the $y(Z)$ region where valence-like IC would cause a large enhancement.

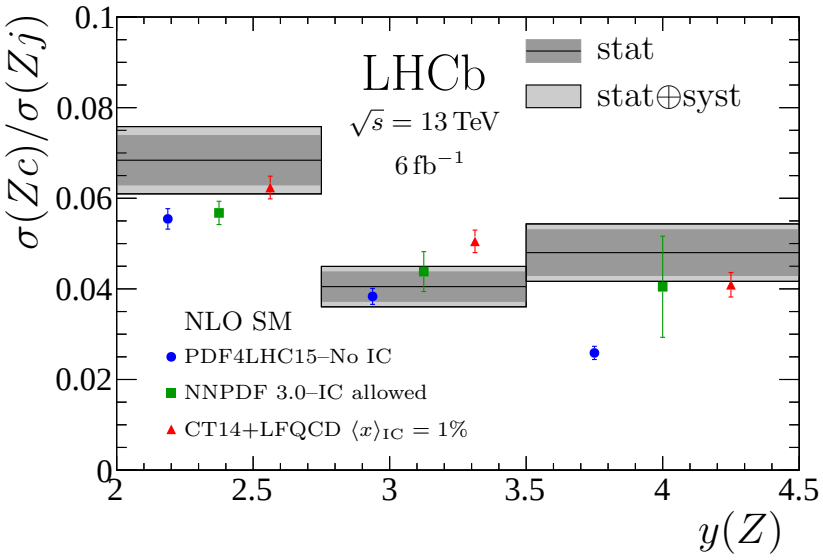

Figure 5: Measured $\mathcal{R}_j^c$ distribution (gray bands) for three intervals of forward Z rapidity, compared to NLO SM predictions [28] without IC [41], with the charm PDF shape allowed to vary (hence, permitting IC) [38, 75], and with IC as predicted by LFQCD with a mean momentum fraction of 1% [37]. The predictions are offset in each interval to improve visibility.

Indeed, Fig. 5 shows that, after including the IC PDF shape predicted by LFQCD with a mean momentum fraction of 1%, the theory predictions are consistent with the data. Incorporating these novel forward $\mathcal{R}_j^c$ results into a global analysis should strongly constrain the large-x charm PDF, both in size and in shape. While the large enhancement in the forward-most $y(Z)$ interval is suggestive of valence-like IC, no definitive statements can be made until the $\mathcal{R}_j^c$ results are included in a global PDF analysis.

In conclusion, the fraction of Z+jet events where the jet is a charm jet is measured for the first time in the forward region of pp collisions. The data sample used corresponds to an integrated luminosity of $6\,\text{fb}^{-1}$ collected at a center-of-mass energy of 13 TeV with the LHCb detector. The ratio $\mathcal{R}_j^c$ is measured in intervals of $y(Z)$ and compared to NLO SM calculations. The observed spectrum exhibits a sizable enhancement at forward Z rapidities, consistent with the effect expected if the proton wave function contains the $|uudc\bar{c}\rangle$ component predicted by LFQCD. Incorporating these results into global PDF analyses could reveal that the proton contains valence-like intrinsic charm.

Acknowledgements

We express our gratitude to our colleagues in the CERN accelerator departments for the excellent performance of the LHC. We thank the technical and administrative staff at the LHCb institutes. We acknowledge support from CERN and from the national agencies: CAPES, CNPq, FAPERJ and FINEP (Brazil); MOST and NSFC (China); CNRS/IN2P3 (France); BMBF, DFG and MPG (Germany); INFN (Italy); NWO (Netherlands); MNiSW and NCN (Poland); MEN/IFA (Romania); MSHE (Russia); MICINN (Spain); SNSF and SER (Switzerland); NASU (Ukraine); STFC (United Kingdom); DOE NP and NSF (USA). We acknowledge the computing resources that are provided by CERN, IN2P3

(France), KIT and DESY (Germany), INFN (Italy), SURF (Netherlands), PIC (Spain), GridPP (United Kingdom), RRCKI and Yandex LLC (Russia), CSCS (Switzerland), IFIN-HH (Romania), CBPF (Brazil), PL-GRID (Poland) and NERSC (USA). We are indebted to the communities behind the multiple open-source software packages on which we depend. Individual groups or members have received support from ARC and ARDC (Australia); AvH Foundation (Germany); EPLANET, Marie Skłodowska-Curie Actions and ERC (European Union); A*MIDEX, ANR, IPhU and Labex P2IO, and Région Auvergne-Rhône-Alpes (France); Key Research Program of Frontier Sciences of CAS, CAS PIFI, CAS CCEPP, Fundamental Research Funds for the Central Universities, and Sci. & Tech. Program of Guangzhou (China); RFBR, RSF and Yandex LLC (Russia); GVA, XuntaGal and GENCAT (Spain); the Leverhulme Trust, the Royal Society and UKRI (United Kingdom).

References

[1] S. J. Brodsky *et al.*, *A review of the intrinsic heavy quark content of the nucleon*, Adv. High Energy Phys. **2015** (2015) 231547, arXiv:1504.06287.

[2] S. J. Brodsky, P. Hoyer, C. Peterson, and N. Sakai, *The intrinsic charm of the proton*, Phys. Lett. **B93** (1980) 451.

[3] S. J. Brodsky, C. Peterson, and N. Sakai, *Intrinsic heavy quark states*, Phys. Rev. **D23** (1981) 2745.

[4] E. Hoffmann and R. Moore, *Subleading contributions to the intrinsic charm of the nucleon*, Z. Phys. **C20** (1983) 71.

[5] F. S. Navarra, M. Nielsen, C. A. A. Nunes, and M. Teixeira, *On the intrinsic charm component of the nucleon*, Phys. Rev. **D54** (1996) 842, arXiv:hep-ph/9504388.

[6] M. Franz, M. V. Polyakov, and K. Goeke, *Heavy quark mass expansion and intrinsic charm in light hadrons*, Phys. Rev. **D62** (2000) 074024, arXiv:hep-ph/0002240.

[7] J. Pumplin, *Light-cone models for intrinsic charm and bottom*, Phys. Rev. **D73** (2006) 114015, arXiv:hep-ph/0508184.

[8] MILC collaboration, W. Freeman and D. Toussaint, *Intrinsic strangeness and charm of the nucleon using improved staggered fermions*, Phys. Rev. **D88** (2013) 054503, arXiv:1204.3866.

[9] S. Brodsky, G. de Teramond, and M. Karliner, *Puzzles in hadronic physics and novel quantum chromodynamics phenomenology*, Ann. Rev. Nucl. Part. Sci. **62** (2012) 1, arXiv:1302.5684.

[10] XQCD collaboration, M. Gong *et al.*, *Strangeness and charmness content of the nucleon from overlap fermions on 2+1-flavor domain-wall fermion configurations*, Phys. Rev. **D88** (2013) 014503, arXiv:1304.1194.

[11] T. J. Hobbs, J. T. Londergan, and W. Melnitchouk, *Phenomenology of nonperturbative charm in the nucleon*, Phys. Rev. **D89** (2014) 074008, arXiv:1311.1578.

[12] R. D. Ball *et al.*, *Intrinsic charm in a matched general-mass scheme*, Phys. Lett. **B754** (2016) 49, arXiv:1510.00009.

[13] S. Duan, C. S. An, and B. Saghai, *Intrinsic charm content of the nucleon and charmness-nucleon sigma term*, Phys. Rev. **D93** (2016) 114006, arXiv:1606.02000.

[14] R. S. Sufian *et al.*, *Constraints on charm-anticharm asymmetry in the nucleon from lattice qcd*, Physics Letters **B808** (2020) 135633.

[15] IceCube collaboration, M. G. Aartsen *et al.*, *Evidence for high-energy extraterrestrial neutrinos at the IceCube detector*, Science **342** (2013) 1242856, arXiv:1311.5238.

[16] R. Gauld *et al.*, *The prompt atmospheric neutrino flux in the light of LHCb*, JHEP **02** (2016) 130, arXiv:1511.06346.

[17] F. Halzen and L. Wille, *Charm contribution to the atmospheric neutrino flux*, Phys. Rev. **D94** (2016) 014014, arXiv:1605.01409.

[18] R. Laha and S. J. Brodsky, *IceCube can constrain the intrinsic charm of the proton*, Phys. Rev. **D96** (2017) 123002, arXiv:1607.08240.

[19] A. V. Giannini, V. P. Gonçalves, and F. S. Navarra, *Intrinsic charm contribution to the prompt atmospheric neutrino flux*, Phys. Rev. **D98** (2018) 014012, arXiv:1803.01728.

[20] V. P. Gonalves, R. Maciula, and A. Szczurek, *Impact of intrinsic charm amount in the nucleon and saturation effects on the prompt atmospheric ν_μ flux for IceCube*, arXiv:2103.05503.

[21] H. L. Lai *et al.*, *The Strange parton distribution of the nucleon: Global analysis and applications*, JHEP **04** (2007) 089, arXiv:hep-ph/0702268.

[22] S. J. Brodsky, A. S. Goldhaber, B. Z. Kopeliovich, and I. Schmidt, *Higgs hadroproduction at large Feynman x*, Nucl. Phys. **B807** (2009) 334, arXiv:0707.4658.

[23] T. P. Stavreva and J. F. Owens, *Direct photon production in association with a heavy quark at hadron colliders*, Phys. Rev. **D79** (2009) 054017, arXiv:0901.3791.

[24] V. A. Bednyakov *et al.*, *Searching for intrinsic charm in the proton at the LHC*, Phys. Lett. **B728** (2014) 602, arXiv:1305.3548.

[25] S. Dulat *et al.*, *Intrinsic charm parton distribution functions from CTEQ-TEA global analysis*, Phys. Rev. **D89** (2014) 073004, arXiv:1309.0025.

[26] F. Halzen, Y. S. Jeong, and C. S. Kim, *Charge asymmetry of weak boson production at the LHC and the charm content of the proton*, Phys. Rev. **D88** (2013) 073013, arXiv:1304.0322.

[27] S. Rostami, A. Khorramian, A. Aleedaneshvar, and M. Goharipour, *The impact of the intrinsic charm quark content of a proton on the differential $\gamma + c$ cross section*, J. Phys. **G43** (2016) 055001, arXiv:1510.08421.

[28] T. Boettcher, P. Ilten, and M. Williams, *Direct probe of the intrinsic charm content of the proton*, Phys. Rev. **D93** (2016) 074008, arXiv:1512.06666.

[29] G. Bailas and V. P. Goncalves, *Phenomenological implications of the intrinsic charm in the Z boson production at the LHC*, Eur. Phys. J. **C76** (2016) 105, arXiv:1512.06007.

[30] A. V. Lipatov, G. I. Lykasov, Y. Y. Stepanenko, and V. A. Bednyakov, *Probing proton intrinsic charm in photon or Z boson production accompanied by heavy jets at the LHC*, Phys. Rev. **D94** (2016) 053011, arXiv:1606.04882.

[31] W. Bai and M. H. Reno, *Prompt neutrinos and intrinsic charm at SHiP*, JHEP **02** (2019) 077, arXiv:1807.02746.

[32] European Muon collaboration, J. J. Aubert *et al.*, *Production of charmed particles in 250-GeV μ^+-iron interactions*, Nucl. Phys. **B213** (1983) 31.

[33] LHCb collaboration, R. Aaij *et al.*, *First measurement of charm production in fixed-target configuration at the LHC*, Phys. Rev. Lett. **122** (2019) 132002, arXiv:1810.07907.

[34] B. W. Harris, J. Smith, and R. Vogt, *Reanalysis of the EMC charm production data with extrinsic and intrinsic charm at NLO*, Nucl. Phys. **B461** (1996) 181, arXiv:hep-ph/9508403.

[35] F. M. Steffens, W. Melnitchouk, and A. W. Thomas, *Charm in the nucleon*, Eur. Phys. J. **C11** (1999) 673, arXiv:hep-ph/9903441.

[36] P. Jimenez-Delgado, T. J. Hobbs, J. T. Londergan, and W. Melnitchouk, *New limits on intrinsic charm in the nucleon from global analysis of parton distributions*, Phys. Rev. Lett. **114** (2015) 082002, arXiv:1408.1708.

[37] T.-J. Hou *et al.*, *CT14 intrinsic charm parton distribution functions from CTEQ-TEA global analysis*, JHEP **02** (2018) 059, arXiv:1707.00657.

[38] NNPDF collaboration, R. D. Ball *et al.*, *A determination of the charm content of the proton*, Eur. Phys. J. **C76** (2016) 647, arXiv:1605.06515.

[39] D0 collaboration, V. M. Abazov *et al.*, *Measurement of associated production of Z bosons with charm quark jets in $p\bar{p}$ collisions at $\sqrt{s} = 1.96$ TeV*, Phys. Rev. Lett. **112** (2014) 042001, arXiv:1308.4384.

[40] CMS collaboration, A. M. Sirunyan *et al.*, *Measurement of the associated production of a Z boson with charm or bottom quark jets in proton-proton collisions at $\sqrt{s}$=13 TeV*, Phys. Rev. **D102** (2020) 032007, arXiv:2001.06899.

[41] J. Butterworth *et al.*, *PDF4LHC recommendations for LHC Run II*, J. Phys. **G43** (2016) 023001, arXiv:1510.03865.

[42] See Supplemental Material at the end of this Letter for details on the theoretical predictions, and for additional plots and numerical results.

[43] M. Cacciari, G. P. Salam, and G. Soyez, *The anti-k_T jet clustering algorithm*, JHEP **0804** (2008) 063, arXiv:0802.1189.

[44] LHCb collaboration, R. Aaij *et al.*, *Identification of charm jets at LHCb in Run 2*, LHCb-DP-2021-006, in preparation.

[45] LHCb collaboration, A. A. Alves Jr. *et al.*, *The LHCb detector at the LHC*, JINST **3** (2008) S08005.

[46] LHCb collaboration, R. Aaij *et al.*, *LHCb detector performance*, Int. J. Mod. Phys. **A30** (2015) 1530022, arXiv:1412.6352.

[47] T. Sjöstrand, S. Mrenna, and P. Skands, *A brief introduction to PYTHIA 8.1*, Comput. Phys. Commun. **178** (2008) 852, arXiv:0710.3820; T. Sjöstrand, S. Mrenna, and P. Skands, *PYTHIA 6.4 physics and manual*, JHEP **05** (2006) 026, arXiv:hep-ph/0603175.

[48] I. Belyaev *et al.*, *Handling of the generation of primary events in Gauss, the LHCb simulation framework*, J. Phys. Conf. Ser. **331** (2011) 032047.

[49] D. J. Lange, *The EvtGen particle decay simulation package*, Nucl. Instrum. Meth. **A462** (2001) 152.

[50] N. Davidson, T. Przedzinski, and Z. Was, *PHOTOS interface in C++: Technical and physics documentation*, Comp. Phys. Comm. **199** (2016) 86, arXiv:1011.0937.

[51] Geant4 collaboration, J. Allison *et al.*, *Geant4 developments and applications*, IEEE Trans. Nucl. Sci. **53** (2006) 270; Geant4 collaboration, S. Agostinelli *et al.*, *Geant4: A simulation toolkit*, Nucl. Instrum. Meth. **A506** (2003) 250.

[52] M. Clemencic *et al.*, *The LHCb simulation application, Gauss: Design, evolution and experience*, J. Phys. Conf. Ser. **331** (2011) 032023.

[53] R. Aaij *et al.*, *The LHCb trigger and its performance in 2011*, JINST **8** (2013) P04022, arXiv:1211.3055.

[54] R. Aaij *et al.*, *Performance of the LHCb trigger and full real-time reconstruction in Run 2 of the LHC*, JINST **14** (2019) P04013, arXiv:1812.10790.

[55] LHCb collaboration, R. Aaij *et al.*, *Study of forward Z +jet production in pp collisions at $\sqrt{s}$ =7 TeV*, JHEP **01** (2014) 033, arXiv:1310.8197.

[56] M. Cacciari, G. P. Salam, and G. Soyez, *FastJet user manual*, Eur. Phys. J. **C72** (2012) 1896, arXiv:1111.6097.

[57] LHCb collaboration, R. Aaij *et al.*, *Identification of beauty and charm quark jets at LHCb*, JINST **10** (2015) P06013, arXiv:1504.07670.

[58] LHCb collaboration, R. Aaij *et al.*, *First observation of top quark production in the forward region*, Phys. Rev. Lett. **115** (2015) 112001, arXiv:1506.00903.

[59] LHCb collaboration, R. Aaij *et al.*, *Study of W boson production in association with beauty and charm*, Phys. Rev. **D92** (2015) 052012, arXiv:1505.04051.

[60] G. D'Agostini, *A multidimensional unfolding method based on Bayes' theorem*, Nucl. Instrum. Meth. **A362** (1995) 487.

[61] T. Adye, *Unfolding algorithms and tests using RooUnfold*, in *PHYSTAT 2011*, (Geneva), 313–318, CERN, 2011, arXiv:1105.1160.

[62] M. Alexander *et al.*, *Mapping the material in the LHCb vertex locator using secondary hadronic interactions*, JINST **13** (2018) P06008, arXiv:1803.07466.

[63] LHCb collaboration, R. Aaij *et al.*, *Study of J/ψ production in jets*, Phys. Rev. Lett. **118** (2017) 192001, arXiv:1701.05116.

[64] Particle Data Group, P. A. Zyla *et al.*, *Review of particle physics*, Prog. Theor. Exp. Phys. **2020** (2020) 083C01.

[65] M. Lisovyi, A. Verbytskyi, and O. Zenaiev, *Combined analysis of charm-quark fragmentation-fraction measurements*, Eur. Phys. J. **C76** (2016) 397, arXiv:1509.01061.

[66] S. Alioli, P. Nason, C. Oleari, and E. Re, *Vector boson plus one jet production in POWHEG*, JHEP **01** (2011) 095, arXiv:1009.5594.

[67] T. Sjöstrand, S. Ask, J. R. Christiansen, R. Corke, N. Desai, P. Ilten, S. Mrenna, S. Prestel, C. O. Rasmussen, and P. Z. Skands, *An introduction to PYTHIA 8.2*, Comput. Phys. Commun. **191** (2015) 159, arXiv:1410.3012.

[68] P. Nason, *A new method for combining NLO QCD with shower Monte Carlo algorithms*, JHEP **11** (2004) 040, arXiv:hep-ph/0409146.

[69] J. Alwall *et al.*, *The automated computation of tree-level and next-to-leading order differential cross sections, and their matching to parton shower simulations*, JHEP **07** (2014) 079, arXiv:1405.0301.

[70] R. Frederix and S. Frixione, *Merging meets matching in MC@NLO*, JHEP **12** (2012) 061, arXiv:1209.6215.

[71] P. Golonka and Z. Was, *PHOTOS Monte Carlo: A precision tool for QED corrections in Z and W decays*, Eur. Phys. J. **C45** (2006) 97, arXiv:hep-ph/0506026.

[72] W. T. Giele and S. Keller, *Implications of hadron collider observables on parton distribution function uncertainties*, Phys. Rev. **D58** (1998) 094023, arXiv:hep-ph/9803393.

[73] J. M. Campbell, R. K. Ellis, and C. Williams, *Vector boson pair production at the LHC*, JHEP **07** (2011) 018, arXiv:1105.0020.

[74] J. M. Campbell, R. K. Ellis, and W. T. Giele, *A multi-threaded version of MCFM*, Eur. Phys. J. **C75** (2015) 246, arXiv:1503.06182.

[75] NNPDF collaboration, R. D. Ball *et al.*, *Parton distributions for the LHC Run II*, JHEP **04** (2015) 040, arXiv:1410.8849.

[76] L. A. Harland-Lang, A. D. Martin, P. Motylinski, and R. S. Thorne, *Parton distributions in the LHC era: MMHT 2014 PDFs*, Eur. Phys. J. **C75** (2015) 204, arXiv:1412.3989.

[77] S. Dulat *et al.*, *New parton distribution functions from a global analysis of quantum chromodynamics*, Phys. Rev. **D93** (2016) 033006, arXiv:1506.07443.

Supplemental Material for LHCb-PAPER-2021-029

Study of Z bosons produced in association with charm in the forward region

Theory Predictions

The NLO SM calculations of Ref. [28] are updated here to use more recent PDFs [37, 38, 41, 75, 76]. These predictions are made using the Zj POWHEGBOX matrix element [66] interfaced to the PYTHIA 8 parton shower [67] using POWHEG matching [68]. These predictions were cross-checked against results produced with the aMC@NLO matrix element generator [69] interfaced to the PYTHIA 8 parton shower using FXFX matching [70]. Hadronization was performed with the PYTHIA 8 event generator, while hadrons were decayed with the EVTGEN package [49] interfaced with the PHOTOS final state radiation generator [71]. The results in Ref. [28] were produced using the CT14 NNLO PDF set [77] for the matrix element, and the corresponding LO PDF set for the parton shower. Using the kinematics of the initiating partons, these results were then weighted in this analysis to produce predictions from more recent PDF sets.

The associated systematic uncertainty for these predictions consists of PDF, scale, and strong-coupling uncertainty. Full correlations were considered when evaluating these uncertainties. The PDF uncertainty is determined using the technique of Monte Carlo PDF replicas [72], while the scale uncertainty is determined from the envelope obtained by independently varying both the factorization and renormalization scales by up to a factor of two. The strong coupling uncertainty is evaluated by varying α_s within experimental uncertainty. Both the scale and strong-coupling uncertainties largely cancel in the ratio, leaving the PDF as the dominant source of uncertainty.

These theory predictions are validated by comparing to the $\mathcal{R}_j^c$ results from the CMS collaboration at central $y(Z)$ [40], where there is minimal sensitivity to IC. The CMS collaboration measured $\mathcal{R}_j^c$ to be $(10.2 \pm 0.9)\%$. Reference [40] also provides NLO SM predictions, $(11.1 \pm 0.3)\%$ and $(9.0 \pm 0.9)\%$, obtained using the aMC@NLO generator interfaced with the PYTHIA 8 parton shower using FXFX matching and the fixed-order MCFM generator [73, 74], respectively. Repeating the procedure used to obtain the theory predictions presented in this Letter, but in the CMS fiducial region, gives $(9.6 \pm 1.0)\%$, $(9.5 \pm 1.0)\%$, and $(9.7 \pm 1.0)\%$ for the PDF4LHC15 no IC, NNPDF 3.0 IC allowed, and CT14 with LFQCD PDFs, respectively. Therefore, the approach used here produces predictions that are consistent both with the CMS measurement and with the theory predictions provided in Ref. [40].

Finally, in Fig. 5 the CT14 with LFQCD results are from the PDF set labeled as BHPS3 in Ref. [37], which is provided for the value $\langle x \rangle_{\rm IC} = 1\%$.

Additional Numerical Results

Numerical results are provided in Table 3. The statistical uncertainties are uncorrelated between $y(Z)$ intervals, whereas the systematic uncertainties are approximately completely correlated. Since many of the systematic uncertainties are correlated between $y(Z)$ intervals, numerical results are also provided for the ratios of $\mathcal{R}_j^c$ values between pairs of intervals in Table S1.

Table S1: Numerical results for the ratios $r_j^c(i/k) \equiv \mathcal{R}_j^c[y(Z)_i]/\mathcal{R}_j^c[y(Z)_k]$, where the first uncertainty is statistical and the second is systematic for each result. The labels low, mid, and high refer to $y(Z)$ ranges of 2.00–2.75, 2.75–3.50 and 3.50–4.50, respectively.

Ratio	Value
r_j^c(mid/low)	$0.59 \pm 0.07 \pm 0.04$
r_j^c(high/low)	$0.70 \pm 0.09 \pm 0.05$
r_j^c(high/mid)	$1.19 \pm 0.16 \pm 0.05$

Additional Figures

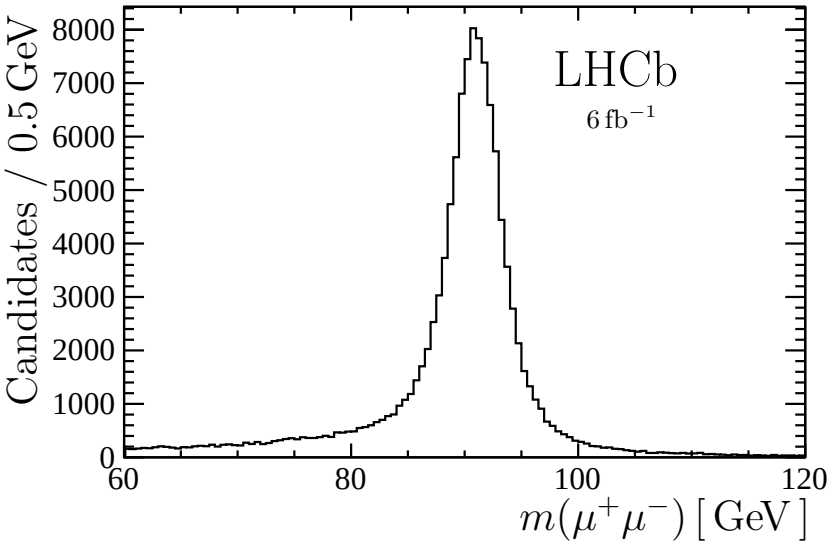

Figure S1: Dimuon invariant mass distribution for the Zj sample.

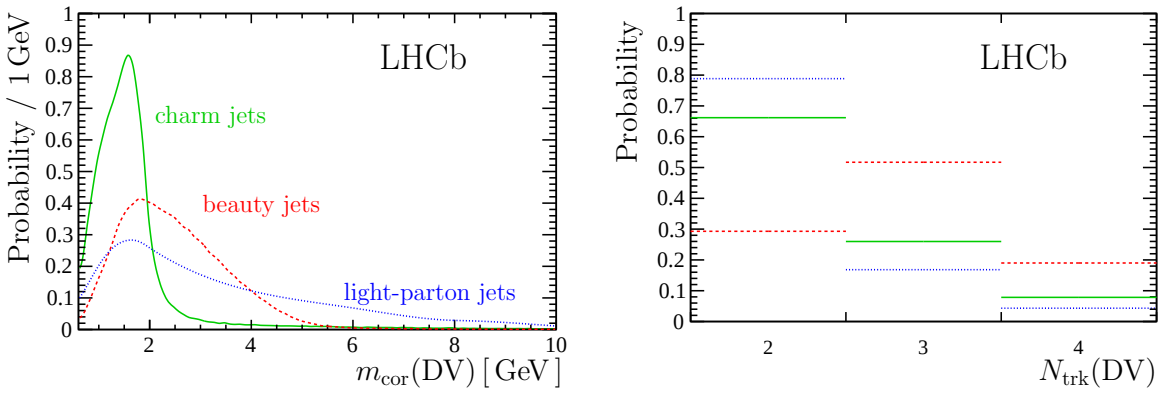

Figure S2: Probability density functions for the DV features used in the c-tagging fits for c, b, and light-parton jets: (left) the corrected mass and (right) the track multiplicity.

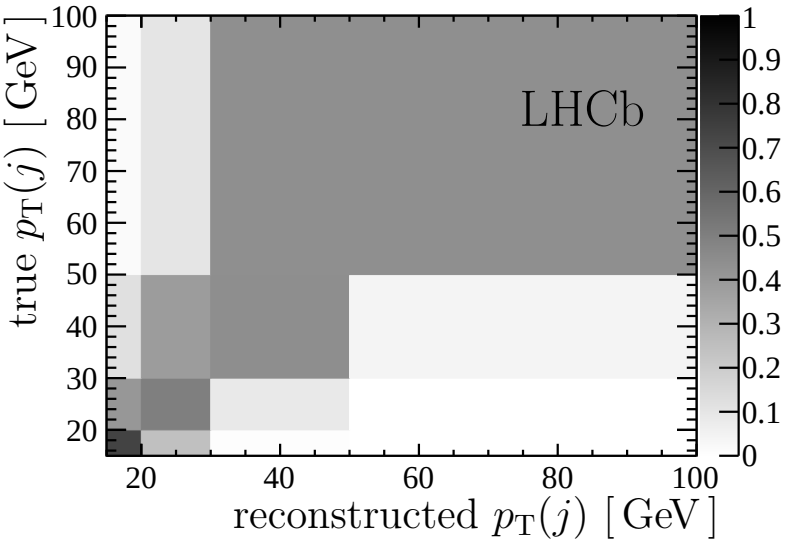

Figure S3: The detector-response matrix for inclusive Zj events. The shading represents the interval-to-interval migration probabilities ranging from (white) 0 to (black) 1. Jets with true (reconstructed) $p_{\rm T}(j)$ in the 20–100 GeV region but for which the reconstructed (true) $p_{\rm T}(j)$ is either below 15 GeV or above 100 GeV are included in the unfolding but not shown graphically.

LHCb collaboration

R. Aaij[32], A.S.W. Abdelmotteleb[56], C. Abellán Beteta[50], F.J. Abudinen Gallego[56], T. Ackernley[60], B. Adeva[46], M. Adinolfi[54], H. Afsharnia[9], C. Agapopoulou[13], C.A. Aidala[87], S. Aiola[25], Z. Ajaltouni[9], S. Akar[65], J. Albrecht[15], F. Alessio[48], M. Alexander[59], A. Alfonso Albero[45], Z. Aliouche[62], G. Alkhazov[38], P. Alvarez Cartelle[55], S. Amato[2], J.L. Amey[54], Y. Amhis[11], L. An[48], L. Anderlini[22], A. Andreianov[38], M. Andreotti[21], F. Archilli[17], A. Artamonov[44], M. Artuso[68], K. Arzymatov[42], E. Aslanides[10], M. Atzeni[50], B. Audurier[12], S. Bachmann[17], M. Bachmayer[49], J.J. Back[56], P. Baladron Rodriguez[46], V. Balagura[12], W. Baldini[21], J. Baptista Leite[1], M. Barbetti[22], R.J. Barlow[62], S. Barsuk[11], W. Barter[61], M. Bartolini[24,h], F. Baryshnikov[83], J.M. Basels[14], S. Bashir[34], G. Bassi[29], B. Batsukh[68], A. Battig[15], A. Bay[49], A. Beck[56], M. Becker[15], F. Bedeschi[29], I. Bediaga[1], A. Beiter[68], V. Belavin[42], S. Belin[27], V. Bellee[50], K. Belous[44], I. Belov[40], I. Belyaev[41], G. Bencivenni[23], E. Ben-Haim[13], A. Berezhnoy[40], R. Bernet[50], D. Berninghoff[17], H.C. Bernstein[68], C. Bertella[48], A. Bertolin[28], C. Betancourt[50], F. Betti[48], Ia. Bezshyiko[50], S. Bhasin[54], J. Bhom[35], L. Bian[73], M.S. Bieker[15], S. Bifani[53], P. Billoir[13], M. Birch[61], F.C.R. Bishop[55], A. Bitadze[62], A. Bizzeti[22,k], M. Bjørn[63], M.P. Blago[48], T. Blake[56], F. Blanc[49], S. Blusk[68], D. Bobulska[59], J.A. Boelhauve[15], O. Boente Garcia[46], T. Boettcher[65], A. Boldyrev[82], A. Bondar[43], N. Bondar[38,48], S. Borghi[62], M. Borisyak[42], M. Borsato[17], J.T. Borsuk[35], S.A. Bouchiba[49], T.J.V. Bowcock[60], A. Boyer[48], C. Bozzi[21], M.J. Bradley[61], S. Braun[66], A. Brea Rodriguez[46], J. Brodzicka[35], A. Brossa Gonzalo[56], D. Brundu[27], A. Buonaura[50], L. Buonincontri[28], A.T. Burke[62], C. Burr[48], A. Bursche[72], A. Butkevich[39], J.S. Butter[32], J. Buytaert[48], W. Byczynski[48], S. Cadeddu[27], H. Cai[73], R. Calabrese[21,f], L. Calefice[15,13], L. Calero Diaz[23], S. Cali[23], R. Calladine[53], M. Calvi[26,j], M. Calvo Gomez[85], P. Camargo Magalhaes[54], P. Campana[23], A.F. Campoverde Quezada[6], S. Capelli[26,j], L. Capriotti[20,d], A. Carbone[20,d], G. Carboni[31], R. Cardinale[24,h], A. Cardini[27], I. Carli[4], P. Carniti[26,j], L. Carus[14], K. Carvalho Akiba[32], A. Casais Vidal[46], G. Casse[60], M. Cattaneo[48], G. Cavallero[48], S. Celani[49], J. Cerasoli[10], D. Cervenkov[63], A.J. Chadwick[60], M.G. Chapman[54], M. Charles[13], Ph. Charpentier[48], G. Chatzikonstantinidis[53], C.A. Chavez Barajas[60], M. Chefdeville[8], C. Chen[3], S. Chen[4], A. Chernov[35], V. Chobanova[46], S. Cholak[49], M. Chrzaszcz[35], A. Chubykin[38], V. Chulikov[38], P. Ciambrone[23], M.F. Cicala[56], X. Cid Vidal[46], G. Ciezarek[48], P.E.L. Clarke[58], M. Clemencic[48], H.V. Cliff[55], J. Closier[48], J.L. Cobbledick[62], V. Coco[48], J.A.B. Coelho[11], J. Cogan[10], E. Cogneras[9], L. Cojocariu[37], P. Collins[48], T. Colombo[48], L. Congedo[19,c], A. Contu[27], N. Cooke[53], G. Coombs[59], I. Corredoira [46], G. Corti[48], C.M. Costa Sobral[56], B. Couturier[48], D.C. Craik[64], J. Crkovská[67], M. Cruz Torres[1], R. Currie[58], C.L. Da Silva[67], S. Dadabaev[83], L. Dai[71], E. Dall'Occo[15], J. Dalseno[46], C. D'Ambrosio[48], A. Danilina[41], P. d'Argent[48], J.E. Davies[62], A. Davis[62], O. De Aguiar Francisco[62], K. De Bruyn[79], S. De Capua[62], M. De Cian[49], J.M. De Miranda[1], L. De Paula[2], M. De Serio[19,c], D. De Simone[50], P. De Simone[23], F. De Vellis[15], J.A. de Vries[80], C.T. Dean[67], F. Debernardis[19,c], D. Decamp[8], V. Dedu[10], L. Del Buono[13], B. Delaney[55], H.-P. Dembinski[15], A. Dendek[34], V. Denysenko[50], D. Derkach[82], O. Deschamps[9], F. Desse[11], F. Dettori[27,e], B. Dey[77], A. Di Cicco[23], P. Di Nezza[23], S. Didenko[83], L. Dieste Maronas[46], H. Dijkstra[48], V. Dobishuk[52], C. Dong[3], A.M. Donohoe[18], F. Dordei[27], A.C. dos Reis[1], L. Douglas[59], A. Dovbnya[51], A.G. Downes[8], M.W. Dudek[35], L. Dufour[48], V. Duk[78], P. Durante[48], J.M. Durham[67], D. Dutta[62], A. Dziurda[35], A. Dzyuba[38], S. Easo[57], U. Egede[69], V. Egorychev[41], S. Eidelman[43,u,†], S. Eisenhardt[58], S. Ek-In[49], L. Eklund[59,86], S. Ely[68], A. Ene[37], E. Epple[67], S. Escher[14], J. Eschle[50], S. Esen[13], T. Evans[48], A. Falabella[20], J. Fan[3], Y. Fan[6], B. Fang[73], S. Farry[60], D. Fazzini[26,j], M. Féo[48], A. Fernandez Prieto[46], A.D. Fernez[66], F. Ferrari[20,d], L. Ferreira Lopes[49], F. Ferreira Rodrigues[2], S. Ferreres Sole[32], M. Ferrillo[50], M. Ferro-Luzzi[48], S. Filippov[39], R.A. Fini[19], M. Fiorini[21,f], M. Firlej[34], K.M. Fischer[63],

D.S. Fitzgerald[87], C. Fitzpatrick[62], T. Fiutowski[34], A. Fkiaras[48], F. Fleuret[12], M. Fontana[13], F. Fontanelli[24,h], R. Forty[48], D. Foulds-Holt[55], V. Franco Lima[60], M. Franco Sevilla[66], M. Frank[48], E. Franzoso[21], G. Frau[17], C. Frei[48], D.A. Friday[59], J. Fu[6], Q. Fuehring[15], E. Gabriel[32], G. Galati[19,c], A. Gallas Torreira[46], D. Galli[20,d], S. Gambetta[58,48], Y. Gan[3], M. Gandelman[2], P. Gandini[25], Y. Gao[5], M. Garau[27], L.M. Garcia Martin[56], P. Garcia Moreno[45], J. García Pardiñas[26,j], B. Garcia Plana[46], F.A. Garcia Rosales[12], L. Garrido[45], C. Gaspar[48], R.E. Geertsema[32], D. Gerick[17], L.L. Gerken[15], E. Gersabeck[62], M. Gersabeck[62], T. Gershon[56], D. Gerstel[10], L. Giambastiani[28], V. Gibson[55], H.K. Giemza[36], A.L. Gilman[63], M. Giovannetti[23,p], A. Gioventù[46], P. Gironella Gironell[45], L. Giubega[37], C. Giugliano[21,f,48], K. Gizdov[58], E.L. Gkougkousis[48], V.V. Gligorov[13], C. Göbel[70], E. Golobardes[85], D. Golubkov[41], A. Golutvin[61,83], A. Gomes[1,a], S. Gomez Fernandez[45], F. Goncalves Abrantes[63], M. Goncerz[35], G. Gong[3], P. Gorbounov[41], I.V. Gorelov[40], C. Gotti[26], E. Govorkova[48], J.P. Grabowski[17], T. Grammatico[13], L.A. Granado Cardoso[48], E. Graugés[45], E. Graverini[49], G. Graziani[22], A. Grecu[37], L.M. Greeven[32], N.A. Grieser[4], L. Grillo[62], S. Gromov[83], B.R. Gruberg Cazon[63], C. Gu[3], M. Guarise[21], M. Guittiere[11], P. A. Günther[17], E. Gushchin[39], A. Guth[14], Y. Guz[44], T. Gys[48], T. Hadavizadeh[69], G. Haefeli[49], C. Haen[48], J. Haimberger[48], T. Halewood-leagas[60], P.M. Hamilton[66], J.P. Hammerich[60], Q. Han[7], X. Han[17], T.H. Hancock[63], E.B. Hansen[62], S. Hansmann-Menzemer[17], N. Harnew[63], T. Harrison[60], C. Hasse[48], M. Hatch[48], J. He[6,b], M. Hecker[61], K. Heijhoff[32], K. Heinicke[15], A.M. Hennequin[48], K. Hennessy[60], L. Henry[48], J. Heuel[14], A. Hicheur[2], D. Hill[49], M. Hilton[62], S.E. Hollitt[15], R. Hou[7], Y. Hou[8], J. Hu[17], J. Hu[72], W. Hu[7], X. Hu[3], W. Huang[6], X. Huang[73], W. Hulsbergen[32], R.J. Hunter[56], M. Hushchyn[82], D. Hutchcroft[60], D. Hynds[32], P. Ibis[15], M. Idzik[34], D. Ilin[38], P. Ilten[65], A. Inglessi[38], A. Ishteev[83], K. Ivshin[38], R. Jacobsson[48], H. Jage[14], S. Jakobsen[48], E. Jans[32], B.K. Jashal[47], A. Jawahery[66], V. Jevtic[15], F. Jiang[3], M. John[63], D. Johnson[48], C.R. Jones[55], T.P. Jones[56], B. Jost[48], N. Jurik[48], S.H. Kalavan Kadavath[34], S. Kandybei[51], Y. Kang[3], M. Karacson[48], M. Karpov[82], F. Keizer[48], D.M. Keller[68], M. Kenzie[56], T. Ketel[33], B. Khanji[15], A. Kharisova[84], S. Kholodenko[44], T. Kirn[14], V.S. Kirsebom[49], O. Kitouni[64], S. Klaver[32], N. Kleijne[29], K. Klimaszewski[36], M.R. Kmiec[36], S. Koliiev[52], A. Kondybayeva[83], A. Konoplyannikov[41], P. Kopciewicz[34], R. Kopecna[17], P. Koppenburg[32], M. Korolev[40], I. Kostiuk[32,52], O. Kot[52], S. Kotriakhova[21,38], P. Kravchenko[38], L. Kravchuk[39], R.D. Krawczyk[48], M. Kreps[56], F. Kress[61], S. Kretzschmar[14], P. Krokovny[43,u], W. Krupa[34], W. Krzemien[36], M. Kucharczyk[35], V. Kudryavtsev[43,u], H.S. Kuindersma[32,33], G.J. Kunde[67], T. Kvaratskheliya[41], D. Lacarrere[48], G. Lafferty[62], A. Lai[27], A. Lampis[27], D. Lancierini[50], J.J. Lane[62], R. Lane[54], G. Lanfranchi[23], C. Langenbruch[14], J. Langer[15], O. Lantwin[83], T. Latham[56], F. Lazzari[29,q], R. Le Gac[10], S.H. Lee[87], R. Lefèvre[9], A. Leflat[40], S. Legotin[83], O. Leroy[10], T. Lesiak[35], B. Leverington[17], H. Li[72], P. Li[17], S. Li[7], Y. Li[4], Y. Li[4], Z. Li[68], X. Liang[68], T. Lin[61], R. Lindner[48], V. Lisovskyi[15], R. Litvinov[27], G. Liu[72], H. Liu[6], Q. Liu[6], S. Liu[4], A. Lobo Salvia[45], A. Loi[27], J. Lomba Castro[46], I. Longstaff[59], J.H. Lopes[2], S. Lopez Solino[46], G.H. Lovell[55], Y. Lu[4], C. Lucarelli[22], D. Lucchesi[28,l], S. Luchuk[39], M. Lucio Martinez[32], V. Lukashenko[32,52], Y. Luo[3], A. Lupato[62], E. Luppi[21,f], O. Lupton[56], A. Lusiani[29,m], X. Lyu[6], L. Ma[4], R. Ma[6], S. Maccolini[20,d], F. Machefert[11], F. Maciuc[37], V. Macko[49], P. Mackowiak[15], S. Maddrell-Mander[54], O. Madejczyk[34], L.R. Madhan Mohan[54], O. Maev[38], A. Maevskiy[82], D. Maisuzenko[38], M.W. Majewski[34], J.J. Malczewski[35], S. Malde[63], B. Malecki[48], A. Malinin[81], T. Maltsev[43,u], H. Malygina[17], G. Manca[27,e], G. Mancinelli[10], D. Manuzzi[20,d], D. Marangotto[25,i], J. Maratas[9,s], J.F. Marchand[8], U. Marconi[20], S. Mariani[22,g], C. Marin Benito[48], M. Marinangeli[49], J. Marks[17], A.M. Marshall[54], P.J. Marshall[60], G. Martelli[78], G. Martellotti[30], L. Martinazzoli[48,j], M. Martinelli[26,j], D. Martinez Santos[46], F. Martinez Vidal[47], A. Massafferri[1], M. Materok[14], R. Matev[48], A. Mathad[50], V. Matiunin[41], C. Matteuzzi[26], K.R. Mattioli[87], A. Mauri[32], E. Maurice[12], J. Mauricio[45], M. Mazurek[48], M. McCann[61], L. Mcconnell[18], T.H. Mcgrath[62], N.T. Mchugh[59], A. McNab[62], R. McNulty[18],

J.V. Mead[60], B. Meadows[65], G. Meier[15], N. Meinert[76], D. Melnychuk[36], S. Meloni[26,j], M. Merk[32,80], A. Merli[25,i], L. Meyer Garcia[2], M. Mikhasenko[48], D.A. Milanes[74], E. Millard[56], M. Milovanovic[48], M.-N. Minard[8], A. Minotti[26,j], L. Minzoni[21,f], S.E. Mitchell[58], B. Mitreska[62], D.S. Mitzel[15], A. Mödden [15], R.A. Mohammed[63], R.D. Moise[61], S. Mokhnenko[82], T. Mombächer[46], I.A. Monroy[74], S. Monteil[9], M. Morandin[28], G. Morello[23], M.J. Morello[29,m], J. Moron[34], A.B. Morris[75], A.G. Morris[56], R. Mountain[68], H. Mu[3], F. Muheim[58,48], M. Mulder[48], D. Müller[48], K. Müller[50], C.H. Murphy[63], D. Murray[62], P. Muzzetto[27,48], P. Naik[54], T. Nakada[49], R. Nandakumar[57], T. Nanut[49], I. Nasteva[2], M. Needham[58], I. Neri[21], N. Neri[25,i], S. Neubert[75], N. Neufeld[48], R. Newcombe[61], E.M. Niel[11], S. Nieswand[14], N. Nikitin[40], N.S. Nolte[64], C. Normand[8], C. Nunez[87], A. Oblakowska-Mucha[34], V. Obraztsov[44], T. Oeser[14], D.P. O'Hanlon[54], S. Okamura[21], R. Oldeman[27,e], F. Oliva[58], M.E. Olivares[68], C.J.G. Onderwater[79], R.H. O'Neil[58], J.M. Otalora Goicochea[2], T. Ovsiannikova[41], P. Owen[50], A. Oyanguren[47], K.O. Padeken[75], B. Pagare[56], P.R. Pais[48], T. Pajero[63], A. Palano[19], M. Palutan[23], Y. Pan[62], G. Panshin[84], A. Papanestis[57], M. Pappagallo[19,c], L.L. Pappalardo[21,f], C. Pappenheimer[65], W. Parker[66], C. Parkes[62], B. Passalacqua[21], G. Passaleva[22], A. Pastore[19], M. Patel[61], C. Patrignani[20,d], C.J. Pawley[80], A. Pearce[48], A. Pellegrino[32], M. Pepe Altarelli[48], S. Perazzini[20], D. Pereima[41], A. Pereiro Castro[46], P. Perret[9], M. Petric[59,48], K. Petridis[54], A. Petrolini[24,h], A. Petrov[81], S. Petrucci[58], M. Petruzzo[25], T.T.H. Pham[68], A. Philippov[42], L. Pica[29,m], M. Piccini[78], B. Pietrzyk[8], G. Pietrzyk[49], M. Pili[63], D. Pinci[30], F. Pisani[48], M. Pizzichemi[26,48,j], Resmi P.K[10], V. Placinta[37], J. Plews[53], M. Plo Casasus[46], F. Polci[13], M. Poli Lener[23], M. Poliakova[68], A. Poluektov[10], N. Polukhina[83,t], I. Polyakov[68], E. Polycarpo[2], S. Ponce[48], D. Popov[6,48], S. Popov[42], S. Poslavskii[44], K. Prasanth[35], L. Promberger[48], C. Prouve[46], V. Pugatch[52], V. Puill[11], H. Pullen[63], G. Punzi[29,n], H. Qi[3], W. Qian[6], J. Qin[6], N. Qin[3], R. Quagliani[49], B. Quintana[8], N.V. Raab[18], R.I. Rabadan Trejo[6], B. Rachwal[34], J.H. Rademacker[54], M. Rama[29], M. Ramos Pernas[56], M.S. Rangel[2], F. Ratnikov[42,82], G. Raven[33], M. Reboud[8], F. Redi[49], F. Reiss[62], C. Remon Alepuz[47], Z. Ren[3], V. Renaudin[63], R. Ribatti[29], S. Ricciardi[57], K. Rinnert[60], P. Robbe[11], G. Robertson[58], A.B. Rodrigues[49], E. Rodrigues[60], J.A. Rodriguez Lopez[74], E.R.R. Rodriguez Rodriguez[46], A. Rollings[63], P. Roloff[48], V. Romanovskiy[44], M. Romero Lamas[46], A. Romero Vidal[46], J.D. Roth[87], M. Rotondo[23], M.S. Rudolph[68], T. Ruf[48], R.A. Ruiz Fernandez[46], J. Ruiz Vidal[47], A. Ryzhikov[82], J. Ryzka[34], J.J. Saborido Silva[46], N. Sagidova[38], N. Sahoo[56], B. Saitta[27,e], M. Salomoni[48], C. Sanchez Gras[32], R. Santacesaria[30], C. Santamarina Rios[46], M. Santimaria[23], E. Santovetti[31,p], D. Saranin[83], G. Sarpis[14], M. Sarpis[75], A. Sarti[30], C. Satriano[30,o], A. Satta[31], M. Saur[15], D. Savrina[41,40], H. Sazak[9], L.G. Scantlebury Smead[63], A. Scarabotto[13], S. Schael[14], S. Scherl[60], M. Schiller[59], H. Schindler[48], M. Schmelling[16], B. Schmidt[48], S. Schmitt[14], O. Schneider[49], A. Schopper[48], M. Schubiger[32], S. Schulte[49], M.H. Schune[11], R. Schwemmer[48], B. Sciascia[23,48], S. Sellam[46], A. Semennikov[41], M. Senghi Soares[33], A. Sergi[24,h], N. Serra[50], L. Sestini[28], A. Seuthe[15], Y. Shang[5], D.M. Shangase[87], M. Shapkin[44], I. Shchemerov[83], L. Shchutska[49], T. Shears[60], L. Shekhtman[43,u], Z. Shen[5], V. Shevchenko[81], E.B. Shields[26,j], Y. Shimizu[11], E. Shmanin[83], J.D. Shupperd[68], B.G. Siddi[21], R. Silva Coutinho[50], G. Simi[28], S. Simone[19,c], N. Skidmore[62], T. Skwarnicki[68], M.W. Slater[53], I. Slazyk[21,f], J.C. Smallwood[63], J.G. Smeaton[55], A. Smetkina[41], E. Smith[50], M. Smith[61], A. Snoch[32], M. Soares[20], L. Soares Lavra[9], M.D. Sokoloff[65], F.J.P. Soler[59], A. Solovev[38], I. Solovyev[38], F.L. Souza De Almeida[2], B. Souza De Paula[2], B. Spaan[15], E. Spadaro Norella[25,i], P. Spradlin[59], F. Stagni[48], M. Stahl[65], S. Stahl[48], S. Stanislaus[63], O. Steinkamp[50,83], O. Stenyakin[44], H. Stevens[15], S. Stone[68], M. Straticiuc[37], D. Strekalina[83], F. Suljik[63], J. Sun[27], L. Sun[73], Y. Sun[66], P. Svihra[62], P.N. Swallow[53], K. Swientek[34], A. Szabelski[36], T. Szumlak[34], M. Szymanski[48], S. Taneja[62], A.R. Tanner[54], M.D. Tat[63], A. Terentev[83], F. Teubert[48], E. Thomas[48], D.J.D. Thompson[53], K.A. Thomson[60], V. Tisserand[9], S. T'Jampens[8], M. Tobin[4], L. Tomassetti[21,f], X. Tong[5], D. Torres Machado[1], D.Y. Tou[13], E. Trifonova[83], C. Trippl[49],

G. Tuci[6], A. Tully[49], N. Tuning[32,48], A. Ukleja[36], D.J. Unverzagt[17], E. Ursov[83], A. Usachov[32], A. Ustyuzhanin[42,82], U. Uwer[17], A. Vagner[84], V. Vagnoni[20], A. Valassi[48], G. Valenti[20], N. Valls Canudas[85], M. van Beuzekom[32], M. Van Dijk[49], H. Van Hecke[67], E. van Herwijnen[83], C.B. Van Hulse[18], M. van Veghel[79], R. Vazquez Gomez[45], P. Vazquez Regueiro[46], C. Vázquez Sierra[48], S. Vecchi[21], J.J. Velthuis[54], M. Veltri[22,r], A. Venkateswaran[68], M. Veronesi[32], M. Vesterinen[56], D. Vieira[65], M. Vieites Diaz[49], H. Viemann[76], X. Vilasis-Cardona[85], E. Vilella Figueras[60], A. Villa[20], P. Vincent[13], F.C. Volle[11], D. Vom Bruch[10], A. Vorobyev[38], V. Vorobyev[43,u], N. Voropaev[38], K. Vos[80], R. Waldi[17], J. Walsh[29], C. Wang[17], J. Wang[5], J. Wang[4], J. Wang[3], J. Wang[73], M. Wang[3], R. Wang[54], Y. Wang[7], Z. Wang[50], Z. Wang[3], Z. Wang[6], J.A. Ward[56], N.K. Watson[53], S.G. Weber[13], D. Websdale[61], C. Weisser[64], B.D.C. Westhenry[54], D.J. White[62], M. Whitehead[54], A.R. Wiederhold[56], D. Wiedner[15], G. Wilkinson[63], M. Wilkinson[68], I. Williams[55], M. Williams[64], M.R.J. Williams[58], F.F. Wilson[57], W. Wislicki[36], M. Witek[35], L. Witola[17], G. Wormser[11], S.A. Wotton[55], H. Wu[68], K. Wyllie[48], Z. Xiang[6], D. Xiao[7], Y. Xie[7], A. Xu[5], J. Xu[6], L. Xu[3], M. Xu[7], Q. Xu[6], Z. Xu[5], Z. Xu[6], D. Yang[3], S. Yang[6], Y. Yang[6], Z. Yang[5], Z. Yang[66], Y. Yao[68], L.E. Yeomans[60], H. Yin[7], J. Yu[71], X. Yuan[68], O. Yushchenko[44], E. Zaffaroni[49], M. Zavertyaev[16,t], M. Zdybal[35], O. Zenaiev[48], M. Zeng[3], D. Zhang[7], L. Zhang[3], S. Zhang[71], S. Zhang[5], Y. Zhang[5], Y. Zhang[63], A. Zharkova[83], A. Zhelezov[17], Y. Zheng[6], T. Zhou[5], X. Zhou[6], Y. Zhou[6], V. Zhovkovska[11], X. Zhu[3], X. Zhu[7], Z. Zhu[6], V. Zhukov[14,40], J.B. Zonneveld[58], Q. Zou[4], S. Zucchelli[20,d], D. Zuliani[28], G. Zunica[62].

[1] *Centro Brasileiro de Pesquisas Físicas (CBPF), Rio de Janeiro, Brazil*
[2] *Universidade Federal do Rio de Janeiro (UFRJ), Rio de Janeiro, Brazil*
[3] *Center for High Energy Physics, Tsinghua University, Beijing, China*
[4] *Institute Of High Energy Physics (IHEP), Beijing, China*
[5] *School of Physics State Key Laboratory of Nuclear Physics and Technology, Peking University, Beijing, China*
[6] *University of Chinese Academy of Sciences, Beijing, China*
[7] *Institute of Particle Physics, Central China Normal University, Wuhan, Hubei, China*
[8] *Univ. Savoie Mont Blanc, CNRS, IN2P3-LAPP, Annecy, France*
[9] *Université Clermont Auvergne, CNRS/IN2P3, LPC, Clermont-Ferrand, France*
[10] *Aix Marseille Univ, CNRS/IN2P3, CPPM, Marseille, France*
[11] *Université Paris-Saclay, CNRS/IN2P3, IJCLab, Orsay, France*
[12] *Laboratoire Leprince-Ringuet, CNRS/IN2P3, Ecole Polytechnique, Institut Polytechnique de Paris, Palaiseau, France*
[13] *LPNHE, Sorbonne Université, Paris Diderot Sorbonne Paris Cité, CNRS/IN2P3, Paris, France*
[14] *I. Physikalisches Institut, RWTH Aachen University, Aachen, Germany*
[15] *Fakultät Physik, Technische Universität Dortmund, Dortmund, Germany*
[16] *Max-Planck-Institut für Kernphysik (MPIK), Heidelberg, Germany*
[17] *Physikalisches Institut, Ruprecht-Karls-Universität Heidelberg, Heidelberg, Germany*
[18] *School of Physics, University College Dublin, Dublin, Ireland*
[19] *INFN Sezione di Bari, Bari, Italy*
[20] *INFN Sezione di Bologna, Bologna, Italy*
[21] *INFN Sezione di Ferrara, Ferrara, Italy*
[22] *INFN Sezione di Firenze, Firenze, Italy*
[23] *INFN Laboratori Nazionali di Frascati, Frascati, Italy*
[24] *INFN Sezione di Genova, Genova, Italy*
[25] *INFN Sezione di Milano, Milano, Italy*
[26] *INFN Sezione di Milano-Bicocca, Milano, Italy*
[27] *INFN Sezione di Cagliari, Monserrato, Italy*
[28] *Universita degli Studi di Padova, Universita e INFN, Padova, Padova, Italy*
[29] *INFN Sezione di Pisa, Pisa, Italy*
[30] *INFN Sezione di Roma La Sapienza, Roma, Italy*
[31] *INFN Sezione di Roma Tor Vergata, Roma, Italy*

[32] *Nikhef National Institute for Subatomic Physics, Amsterdam, Netherlands*
[33] *Nikhef National Institute for Subatomic Physics and VU University Amsterdam, Amsterdam, Netherlands*
[34] *AGH - University of Science and Technology, Faculty of Physics and Applied Computer Science, Kraków, Poland*
[35] *Henryk Niewodniczanski Institute of Nuclear Physics Polish Academy of Sciences, Kraków, Poland*
[36] *National Center for Nuclear Research (NCBJ), Warsaw, Poland*
[37] *Horia Hulubei National Institute of Physics and Nuclear Engineering, Bucharest-Magurele, Romania*
[38] *Petersburg Nuclear Physics Institute NRC Kurchatov Institute (PNPI NRC KI), Gatchina, Russia*
[39] *Institute for Nuclear Research of the Russian Academy of Sciences (INR RAS), Moscow, Russia*
[40] *Institute of Nuclear Physics, Moscow State University (SINP MSU), Moscow, Russia*
[41] *Institute of Theoretical and Experimental Physics NRC Kurchatov Institute (ITEP NRC KI), Moscow, Russia*
[42] *Yandex School of Data Analysis, Moscow, Russia*
[43] *Budker Institute of Nuclear Physics (SB RAS), Novosibirsk, Russia*
[44] *Institute for High Energy Physics NRC Kurchatov Institute (IHEP NRC KI), Protvino, Russia, Protvino, Russia*
[45] *ICCUB, Universitat de Barcelona, Barcelona, Spain*
[46] *Instituto Galego de Física de Altas Enerxías (IGFAE), Universidade de Santiago de Compostela, Santiago de Compostela, Spain*
[47] *Instituto de Fisica Corpuscular, Centro Mixto Universidad de Valencia - CSIC, Valencia, Spain*
[48] *European Organization for Nuclear Research (CERN), Geneva, Switzerland*
[49] *Institute of Physics, Ecole Polytechnique Fédérale de Lausanne (EPFL), Lausanne, Switzerland*
[50] *Physik-Institut, Universität Zürich, Zürich, Switzerland*
[51] *NSC Kharkiv Institute of Physics and Technology (NSC KIPT), Kharkiv, Ukraine*
[52] *Institute for Nuclear Research of the National Academy of Sciences (KINR), Kyiv, Ukraine*
[53] *University of Birmingham, Birmingham, United Kingdom*
[54] *H.H. Wills Physics Laboratory, University of Bristol, Bristol, United Kingdom*
[55] *Cavendish Laboratory, University of Cambridge, Cambridge, United Kingdom*
[56] *Department of Physics, University of Warwick, Coventry, United Kingdom*
[57] *STFC Rutherford Appleton Laboratory, Didcot, United Kingdom*
[58] *School of Physics and Astronomy, University of Edinburgh, Edinburgh, United Kingdom*
[59] *School of Physics and Astronomy, University of Glasgow, Glasgow, United Kingdom*
[60] *Oliver Lodge Laboratory, University of Liverpool, Liverpool, United Kingdom*
[61] *Imperial College London, London, United Kingdom*
[62] *Department of Physics and Astronomy, University of Manchester, Manchester, United Kingdom*
[63] *Department of Physics, University of Oxford, Oxford, United Kingdom*
[64] *Massachusetts Institute of Technology, Cambridge, MA, United States*
[65] *University of Cincinnati, Cincinnati, OH, United States*
[66] *University of Maryland, College Park, MD, United States*
[67] *Los Alamos National Laboratory (LANL), Los Alamos, United States*
[68] *Syracuse University, Syracuse, NY, United States*
[69] *School of Physics and Astronomy, Monash University, Melbourne, Australia, associated to* [56]
[70] *Pontifícia Universidade Católica do Rio de Janeiro (PUC-Rio), Rio de Janeiro, Brazil, associated to* [2]
[71] *Physics and Micro Electronic College, Hunan University, Changsha City, China, associated to* [7]
[72] *Guangdong Provincial Key Laboratory of Nuclear Science, Guangdong-Hong Kong Joint Laboratory of Quantum Matter, Institute of Quantum Matter, South China Normal University, Guangzhou, China, associated to* [3]
[73] *School of Physics and Technology, Wuhan University, Wuhan, China, associated to* [3]
[74] *Departamento de Fisica , Universidad Nacional de Colombia, Bogota, Colombia, associated to* [13]
[75] *Universität Bonn - Helmholtz-Institut für Strahlen und Kernphysik, Bonn, Germany, associated to* [17]
[76] *Institut für Physik, Universität Rostock, Rostock, Germany, associated to* [17]
[77] *Eotvos Lorand University, Budapest, Hungary, associated to* [48]
[78] *INFN Sezione di Perugia, Perugia, Italy, associated to* [21]
[79] *Van Swinderen Institute, University of Groningen, Groningen, Netherlands, associated to* [32]
[80] *Universiteit Maastricht, Maastricht, Netherlands, associated to* [32]

[81] *National Research Centre Kurchatov Institute, Moscow, Russia, associated to* [41]
[82] *National Research University Higher School of Economics, Moscow, Russia, associated to* [42]
[83] *National University of Science and Technology "MISIS", Moscow, Russia, associated to* [41]
[84] *National Research Tomsk Polytechnic University, Tomsk, Russia, associated to* [41]
[85] *DS4DS, La Salle, Universitat Ramon Llull, Barcelona, Spain, associated to* [45]
[86] *Department of Physics and Astronomy, Uppsala University, Uppsala, Sweden, associated to* [59]
[87] *University of Michigan, Ann Arbor, United States, associated to* [68]

[a] *Universidade Federal do Triângulo Mineiro (UFTM), Uberaba-MG, Brazil*
[b] *Hangzhou Institute for Advanced Study, UCAS, Hangzhou, China*
[c] *Università di Bari, Bari, Italy*
[d] *Università di Bologna, Bologna, Italy*
[e] *Università di Cagliari, Cagliari, Italy*
[f] *Università di Ferrara, Ferrara, Italy*
[g] *Università di Firenze, Firenze, Italy*
[h] *Università di Genova, Genova, Italy*
[i] *Università degli Studi di Milano, Milano, Italy*
[j] *Università di Milano Bicocca, Milano, Italy*
[k] *Università di Modena e Reggio Emilia, Modena, Italy*
[l] *Università di Padova, Padova, Italy*
[m] *Scuola Normale Superiore, Pisa, Italy*
[n] *Università di Pisa, Pisa, Italy*
[o] *Università della Basilicata, Potenza, Italy*
[p] *Università di Roma Tor Vergata, Roma, Italy*
[q] *Università di Siena, Siena, Italy*
[r] *Università di Urbino, Urbino, Italy*
[s] *MSU - Iligan Institute of Technology (MSU-IIT), Iligan, Philippines*
[t] *P.N. Lebedev Physical Institute, Russian Academy of Science (LPI RAS), Moscow, Russia*
[u] *Novosibirsk State University, Novosibirsk, Russia*

[†] *Deceased*